Available at www.sciencedirect.com

ScienceDirect

journal homepage: www.elsevier.com/locate/he

Hydrogen storage in zeolite imidazolate frameworks. A multiscale theoretical investigation

*Bassem Assfour, Stefano Leoni, Sergei Yurchenko, Gotthard Seifert**

Technische Universität Dresden, Institut für Physikalische Chemie und Elektrochemie, Bergstr. 66b, D-01062 Dresden, Germany

ARTICLE INFO

Article history:
Received 25 August 2010
Received in revised form
7 February 2011
Accepted 8 February 2011
Available online 12 March 2011

Keywords:
Hydrogen storage
ZIFs
MP2
GCMC

ABSTRACT

A multiscale approach is used to investigate the hydrogen adsorption in nanoporous Zeolite Imidazolate Frameworks (ZIFs) on varying geometries and organic linkers. Ab initio calculations are performed at the MP2 level to obtain correct interaction energies between hydrogen molecules and the ZIF structures. Subsequently, classical grand canonical Monte-Carlo (GCMC) simulations are carried out to obtain the hydrogen uptake of ZIFs at different thermodynamic conditions of pressure and temperature.

1. Introduction

In the perspective of a rapid exhaustion of hydrocarbon resources, hydrogen has been indicated as sustainable 'clean' fuel, optimally suited for transportation applications. Besides sourcing, storage remains one of the principal limiting factor for an economy based on hydrogen. Porous materials are capable of storing practical amounts of hydrogen [1–9]. However, no material yet fully meets the recommendations of the U.S. Department of Energy for reversible hydrogen storage under near ambient conditions. Recently, zeolitic imidazolate frameworks (ZIFs) have appeared as a novel class of materials [10]. Their crystal structure is based on aluminosilicate zeolite nets, whereby the tetrahedral Si(Al) sites are replaced by transition metals M (M = Zn(II), Co(II), In(III)) tetrahedrally coordinated by imidazolate ligands (Fig. 1). Like metal-organic framework (MOF) materials, ZIFs exhibit high porosity and chemical functionality with the advantages of exceptional chemical stability and large structural diversity [11]. The combination of these features makes ZIFs promising candidates for hydrogen storage applications.

ZIF-8 (SOD topology) and ZIF-11 (RHO topology) contain only one cage type, and result from organic linkers 2-methylimidazolate (mIM) and benzimidazolate (bIM) [10] (for the description of topology symbols, see Database of Zeolite Structures, http://www.iza-structure.org/databases/). The more involved LTA topology of ZIF-20, which has two cage types, can be obtained by linker functionalization [12]. Yaghi *et al.* synthesized ZIF-95, with an unprecedented topology (denoted by poz) [13]. ZIF-95 features a tetragonal, neutral framework made of 128 Zn nodes tetrahedrally coordinated by chlorobenzimidazolate (cbIM). It has two types of cages (A and B) with remarkably large pore sizes of 25.1 × 14.3 Å and 30.1 × 20.0 Å, respectively.

Unlike MOFs, only few experimental studies concerning hydrogen storage in ZIFs have been reported so far [10,12,14,15]. Yildirim *et al.* measured the adsorption isotherm of ZIF-8 over a wide range of pressures and temperatures.

* *Corresponding author*. Tel.: +49 351 463 37637; fax: +49 351 463 35953.
E-mail address: Gotthard.Seifert@chemie.tu-dresden.de (G. Seifert).

0360-3199/$ – see front matter Copyright © 2011, Hydrogen Energy Publications, LLC. Published by Elsevier Ltd. All rights reserved.
doi:10.1016/j.ijhydene.2011.02.044

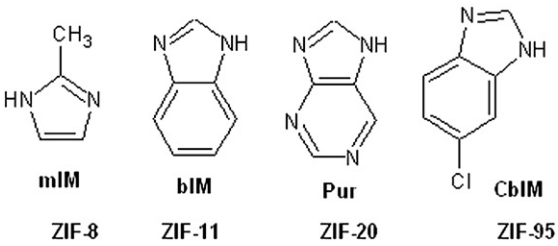

Fig. 1 – Imidazole-type linkers in ZIFs.

At low temperatures the maximum of H_2 adsorption capacity amounts to 4.4 wt% [15].

In coordination with experiments, some theoretical studies of H_2 adsorption on ZIFs have been reported. Wang *et al.* [16] used the refined OPLS-AA (Optimized Potentials for Liquid Simulations-All Atoms) force field model in grand canonical Monte Carlo (GCMC) simulations to investigate the adsorption sites using computer tomography (mCT) techniques. A combination of the Dreiding [17] and the all-atom OPLS (OPLS-AA) [18] force fields was adopted to describe the atomic interactions in the ZIF-8 framework. Fröba *et al.* [19] approached the adsorption of hydrogen in ZIF-8 with the Universal Force Field (UFF).

Recently, Han et al. [20] reported H_2 uptakes of 10 different ZIFs, based on GCMC simulations. The GCMC results show a good agreement with an experimental data set of ZIF-8. Therein, the force fields used to describe the interactions between H_2 and ZIF were based on ab initio calculations. However, the interaction terms between H_2 and Nitrogen in different imidazolate rings were developed from the interaction between H_2 and $C_3N_3H_3$, which is different from imidazolate rings.

The large numbers of GCMC moves requires a prompt calculation of intermolecular forces, made possible by versatile force field parameters. Although general potentials can describe the adsorption effects rather well, sometimes they may lead to unpredictable results for certain materials. On the other hand, tuning force field parameters for a particular compound may impair property prediction upon transferring these parameters to different systems.

To provide a fundamental understanding of adsorption mechanisms in ZIFs and to achieve a more accurate prediction of H_2 storage capacity we have constructed a force field from first-principles. This force field is employed to study H_2

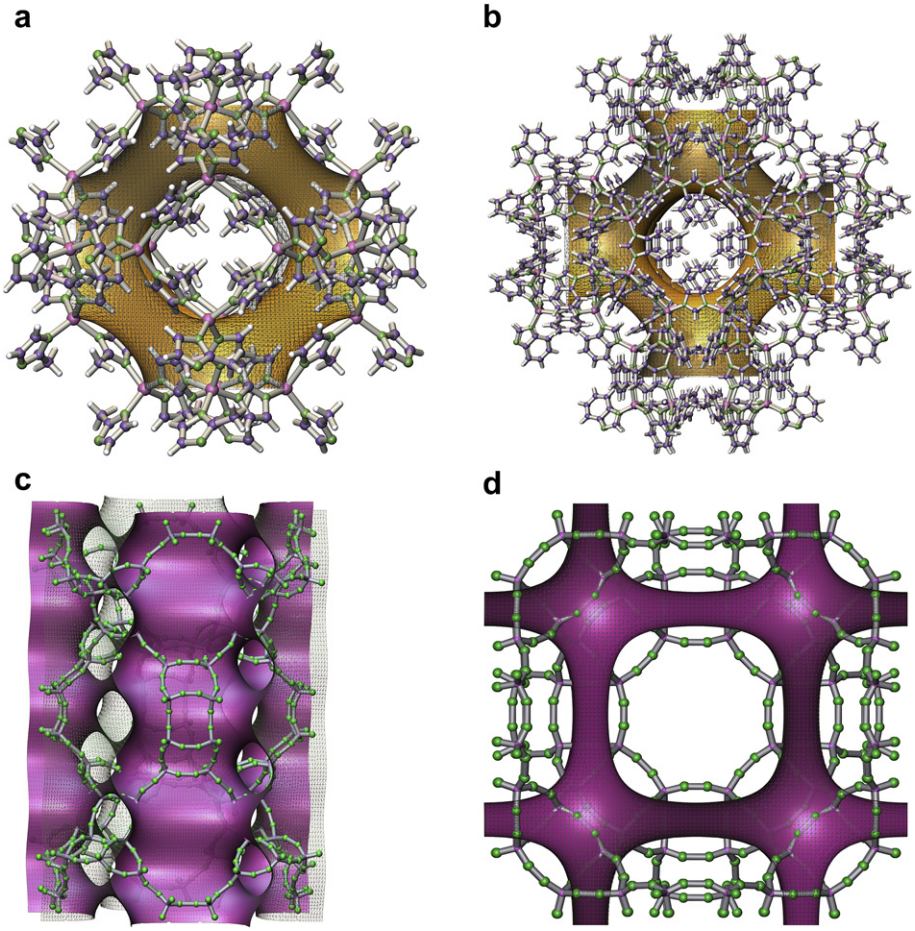

Fig. 2 – Crystal structures of the ZIFs considered in the study: a) ZIF-8, b) ZIF-11 (same topology for ZIF-20) and c) ZIF-95 side and d) top view. The topology of the framework is made explicitly by a minimal surface. Zinc, Carbon, Nitrogen and Hydrogen atoms are shown in pink, blue, green, and white, respectively. For ZIF-95 (c,d) only the Zn-N framework is shown, for clarity. Figure a) and b) are adapted from Ref. [27]. (For interpretation of the references to colour in this figure legend, the reader is referred to the web version of this article.)

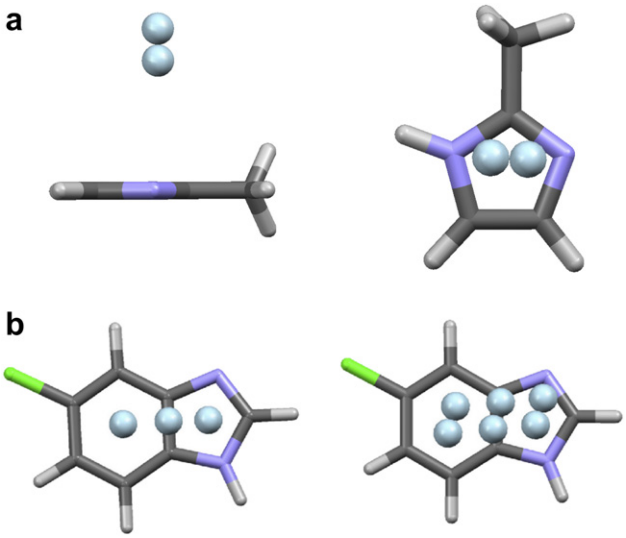

Fig. 3 – Examples of the cluster model used to represent the atom types in ZIF-8(a) and ZIF-95(b) together with the H_2 molecule in different positions and orientations. White, gray, blue and green denote H, C, N, and Cl, respectively. The H_2 molecules are shown in light blue colour. (For interpretation of the references to colour in this figure legend, the reader is referred to the web version of this article.)

storage in ZIF materials with different topologies and different organic linkers. We focus on four main topologies, SOD (ZIF-8), RHO (ZIF-11), LTA (ZIF-20) and POZ (ZIF-95) (see Fig. 2), which have shown promising hydrogen storage properties [10,12]. All structures have the same metal ion (Zn^{2+}) but differ in the imidazolate linkers. This selection allows us to closely investigate the effect of varying topology and organic linkers on the hydrogen adsorption properties of the ZIF materials.

We used second-order Møller-Plesset (MP2) [21] calculations to construct the force field towards an accurate description of the interactions between H_2 and ZIF structures. This force field was then used in grand canonical Monte Carlo (GCMC) simulations to quantitatively predict the H_2 isotherms under different thermodynamic conditions.

2. Computational methodology

2.1. First-principle calculations of interaction parameters

The interactions between H_2 and ZIFs framework are dominated by long-range London dispersion terms, which are known to be problematic for Density Functional Theory (DFT) methods [22]. The MP2 ab initio method together with the cc-PVTZ [23] basis set were chosen to represent the interactions between ZIF frameworks and an H_2 molecule. This level of theory is known to provide appropriate values for the interaction between H_2 and aromatic systems [24–26].

At the MP2 level the full periodic ZIF systems tend to be prohibitively expensive due to the large size of ZIFs. A viable compromise between computational costs and accuracy can be achieved by using a smaller, computationally tractable cluster, representative for the system.

Experimental and theoretical studies of hydrogen adsorption in ZIF-8 indicate that the imidazolate linker is the primary adsorption site for hydrogen [14,16,27], while no adsorption takes place around the Zn-N_4 cluster. Along this line, in MP2 calculations we consider only the interaction between hydrogen and ligands, as shown in Fig. 3(a). For each ZIF the corresponding organic linkers, saturated with hydrogen atoms, were used as reduced clusters (see Fig. 1).

All geometries were first optimized at the B3LYP/6-311G** level and then used in the MP2 calculations. The calculated binding energies were corrected for the basis-set superposition error (BSSE) by the full counterpoise procedure. The calculations were carried out with the Gaussian-03 program package [28].

2.2. Parametrization of the force field

The H_2-ZIF interactions were represented by the 12-6 Lennard-Jones (LJ) potential:

$$V(r_{ij}) = 4\varepsilon_{ij}\left[\left(\frac{\sigma_{ij}}{r_{ij}}\right)^{12} - \left(\frac{\sigma_{ij}}{r_{ij}}\right)^{6}\right], \quad (1)$$

constructed through a least-square fitting to the MP2 energies. Here i and j run over all atoms of the guest (hydrogen molecules) and of the host (ZIF structure), r_{ij} is an atom–atom

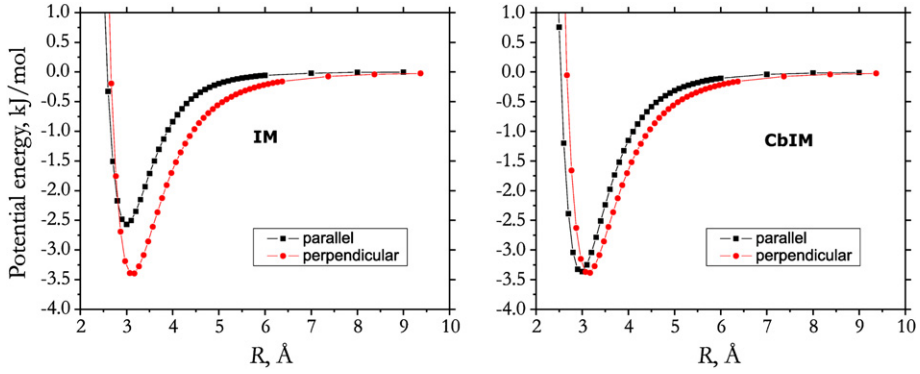

Fig. 4 – Potential energies of H_2 derived from the MP2 calculations on IM (left) and cbIM (right) with H_2 axis parallel and perpendicular to the plane. The R is defined as the distance between the center of mass of the cluster and the center of the H_2 molecule.

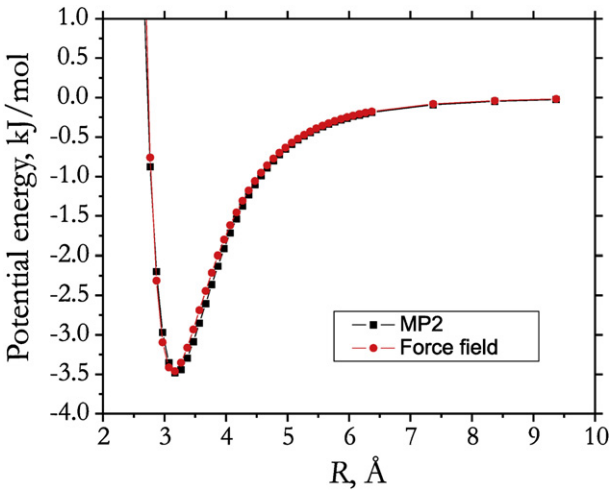

Fig. 5 – Potential energies derived from the MP2 calculations of H_2 on cbIM ring together with the fitted force fields. The distance R is defined as the distance between the center of mass of the cluster and the center of the H_2 molecule.

distance, and σ_{ij} and ε_{ij} are the Lennard–Jones parameters. A similar approach has been successfully used in the literature to fit van der Waals interactions for MOF systems [3,29].

The MP2 energies for ZIF-8 sensibly depends on the H_2 relative orientation with respect to the structure (Fig. 4). In order to take these effects into account, two H_2 limiting orientations were considered, vertical and parallel with respect to the ligands, as shown in Fig. 3(a).

For ZIF-11, –20 and –95, three different H_2 placements were evaluated, at the center of the imidazolate (IM) ring, at the center of the benzene ring and on the top of the C–C bond between IM and benzene rings, respectively [see Fig. 3(b)].

The potential energy profile used in the fitting of the force field parameters corresponded to the most 'favorable' (i.e. with lowest energy) orientations. This choice of the potential profile ensures a good description of the strongest adsorption sites. As a representative, Fig. 5 shows the potential energies derived from the MP2 calculations together with the fitted force fields of H_2 on cbIM.

The H_2–H_2 potential was taken from Ref. [30], where each H atom in an H_2 molecule is represented separately in the LJ potential ($\sigma = 2.72$ Å, $\varepsilon = 10.0$ K). These parameters were shown to provide a reasonably good reproduction of the experimental data of the hydrogen gas. They have been also utilized to simulate the hydrogen adsorption in MOFs [31,34] and COFs [8].

2.3. Simulated adsorption isotherms of H_2

The hydrogen adsorption in the ZIF structures was simulated with GCMC using the multipurpose simulation code Music [32]. The sorbents (ZIFs) were described by a periodic $2 \times 2 \times 2$ supercell to eliminate boundary effects. ZIFs were treated as rigid structures at all temperatures, using coordinates obtained by X-ray scattering experiments [10,12,13]. A cut-off of 13.0 Å was applied to the Lennard–Jones interactions. The calculations of adsorption isotherms were carried out at two different temperatures, $T = 77$ K and 300 K, throughout a wide range of pressure, from low pressure ($P = 10^{-2}$ bar) up to high pressure (P = 100 bar) to get a complete picture of the adsorption properties. For each point on the isotherm, the

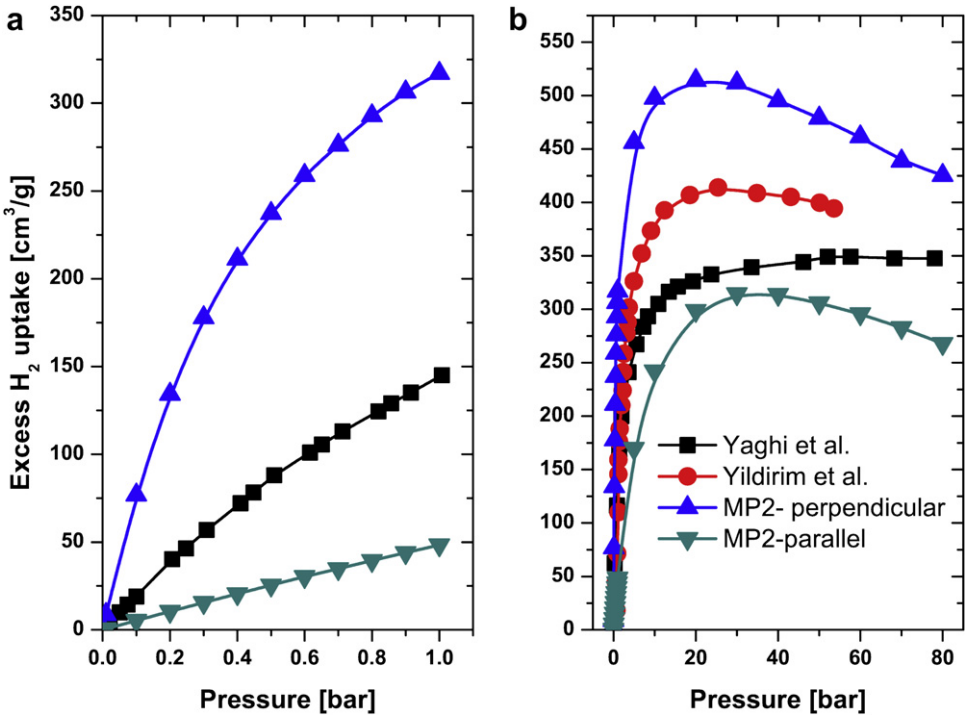

Fig. 6 – Simulated and experimental adsorption isotherm of ZIF-8: a) P = 0–1 bar; b) P = 0–80 bar. The experimental data are taken from Yaghi et al. [10] (squares) and Yildirim et al. [15] (circles).

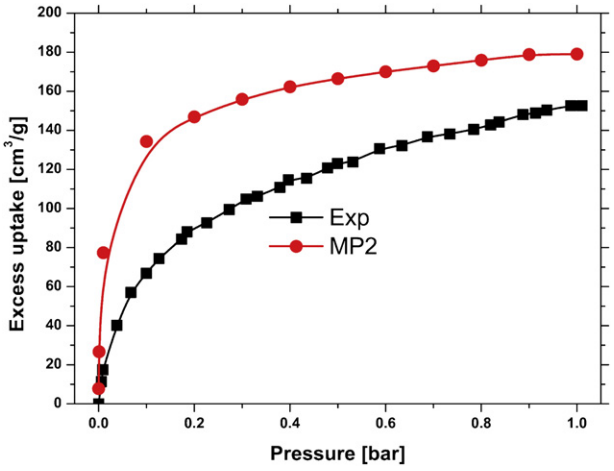

Fig. 7 – Simulated (circles) and experimental (squares) adsorption isotherm of ZIF-11. The experimental data are taken from Ref. [10].

simulations were equilibrated for five million steps, and further five million steps were used to sample the data. Each Monte Carlo step consisted of (i) insertion of a new molecule, (ii) deletion of an existing molecule, (iii) translation, or (iv) rotation of an existing molecule, with equal probabilities.

The isosteric heat of adsorption Q_{st} was evaluated through the fluctuations over the number of particles in the system and fluctuations of the internal energy U [33,34]:

$$Q_{st} = RT - \frac{\langle UN\rangle - \langle U\rangle\langle N\rangle}{\langle N^2\rangle - \langle N\rangle^2} \quad (2)$$

where R is the gas constant, T is the temperature, U is the internal energy, N is the number of molecules adsorbed, and the brackets <…> represent a configuration average.

The available free volume was calculated using a non-adsorbing species (helium) as a probe, while the surface area was obtained by 'rolling' a probe molecule with a diameter equal to the Lennard–Jones parameter for H_2 or N_2 (2.72, 3.68 Å) over the framework surface as described in Ref. [35].

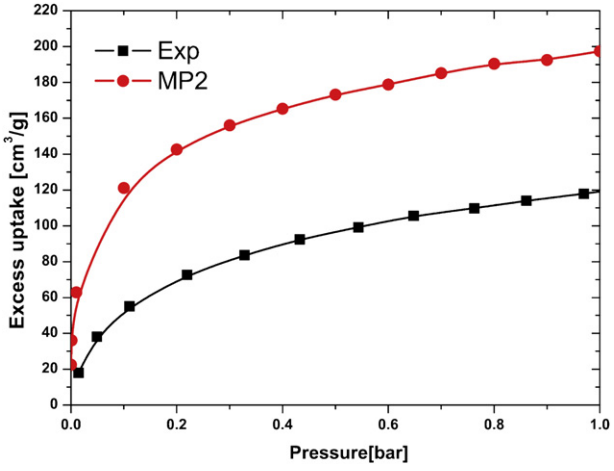

Fig. 8 – Simulated (circles) and experimental (squares) adsorption isotherm of ZIF-20. The experimental data are taken from Ref. [12].

3. Results and discussion

3.1. Comparison of simulations with experiments for H_2 adsorption

To our knowledge, in the literature there are only two experimental data of the adsorption isotherms for ZIF-8 by Yaghi *et al.* [10] and by Yildirim *et al.* [15]. These isotherms, however, display striking differences, with respect to the maximal H_2 uptake as well as the shape of the isotherms (see Fig. 6).

The simulation approach taken in this work consists of evaluating isotherms based on interaction energies obtained from accurate MP2 calculations. This provides a theoretical parameter-free reference, which can be contrasted with available experimental data. Based on this approach, H_2 adsorption isotherms were evaluated for ZIF-8, ZIF-11 and ZIF-20 at $T = 77$ K. The calculated and experimental adsorption isotherms for ZIF-8 are compared in Fig. 6.

The calculated H_2 isotherm curve (blue triangles) displays a cusp around 20 bar. This feature is also present in the measurements of Yildirim *et al.* [15], but not in the experimental curve of Yaghi *et al.* [10], which saturates around 50 bar. This feature, as well as the different curve shape most probably reflects material artifacts, like the presence of solvent molecules and contaminants in pores.

In Fig. 6 a second calculated isotherm for ZIF-8 (grey triangles, Fig. 6) is included. This was obtained from parameters fitted to MP2 energies of the less favorable, parallel orientation of H_2 on the substrate (black potential energy curve in Fig. 4). The two isotherms enclose the experimental region at full range of pressure. The use of the parallel hydrogen orientation leads to an underestimation of the amount of H_2 adsorbed, and an overall bad description of the complex adsorption process. Instead, using the profile of the lowest energy leads to a superior description of the experimental curve, especially for the low pressures, at the highest pressure, and with respect to the maximum placement. Given the difference between the two potential curves (Fig. 4) for ZIF-8, considering only the vertical orientation may in principle add an extra contribution, but only to the weakly adsorbed molecules in the intermediate pressure range. Nonetheless, since the features of the experimental curve are closely reproduced and the adsorption energy is accurately calculated (see below), we consider our parametrization approach reasonable.

Discrepancies between the theoretical and experimental adsorption in porous materials are frequently encountered in the literature (see for example Refs. [7,33,36,37]). Simulation of H_2 uptake on ZIF-8 using the universal force field (UFF) cannot satisfactorily reproduce the experiments [19]. Only upon adjustment of the OPLS-AA force field parameters a better agreement was obtained [16]. Experiments on H_2 adsorption are often affected by the presence of solvent or other guest molecules in pores, which results in an incomplete volume activation of the material causing an inferior H_2 uptake performance. Since we intend to capture the adsorption process in detail based on the first-principles, we understand the calculated curves as benchmark at which the material can nominally perform.

Table 1 – Structural characteristics of ZIF materials calculated from single crystal X-ray analysis. The experimental values are given in parenthesis.

Material	Void fraction (%)	Free volume (cm^3/g)	Accessible Surface area for H_2 (m^2/g)	Accessible Surface area for N_2 (m^2/g)
ZIF-8	55.8	0.568 (0.636[10])	1679	1263 (1630 [10])
ZIF-11	53.7	0.496	1452	610
ZIF-20	53.3	0.479 (0.27 [12])	1430	941 (800 [12])
ZIF-95	60.0	0.628 (0.43 [13])	1635	1251 (1240 [13])

The calculated adsorption isotherm of ZIF-11 and ZIF-20 are shown in Fig. 7 and Fig. 8, respectively, where they are compared to the corresponding experimental isotherms [10], available for the lower pressure region only. The theoretical isotherms are in fairly good agreement with the experiments and are approaching the experimental curves at higher pressure. Similarly to ZIF-8, the MP2 curves lie above the experimental one and represent the maximal uptake when the whole pore volume is accessible. In case of ZIF-20 the experimental free volume is smaller than the theoretical one calculated from a perfect crystal structure (Table 1, third column), which results in a lower placement of the experimental isotherm. We would like to mention that ZIF-11 provides a very small surface area for N_2 compared to H_2. This is consistent with the experimental observation of Yaghi et al. [10], in which ZIF-11 was found not porous to N_2 because its aperture size (3.0 Å) was smaller than the kinetic diameter of nitrogen (3.6 Å); nonetheless, it was able to adsorb hydrogen.

To complement our hydrogen adsorption analysis we have also performed a comparison of hydrogen adsorption in different ZIFs detailed in the next section.

3.2. Comparison between different ZIFs

In order to examine the performance of ZIFs for hydrogen storage, the adsorption isotherms were calculated both at the cryogenic (77 K) and ambient (300 K) temperatures. Fig. 9 shows the predicted total gravimetric H_2 uptakes at 77 K for the ZIFs under consideration at low and high pressure. The total hydrogen uptake of ZIF-8 at moderate and high pressure (>10 bar) is the highest with ~5 wt% at 100 bar (Fig. 9(a)). This can be attributed to the larger surface area and higher free volume of the system (see Table 1). At low pressure (<0.5 bar) ZIF-20 exhibits the highest uptake, while the isotherms of ZIF-11 and ZIF-95 are very close. The initial hydrogen uptake (at very low pressure) for ZIF-20 is much higher than that of ZIF-8 and comparable to that of ZIF-11. This can be attributed to the higher heat of adsorption of ZIF-20 (see Fig. 12). This finding is in agreement with the experimental observation of Yaghi *et al.* [10,12], who also showed that the initial uptake of ZIF-20 is significantly higher than that of ZIF-8. The adsorption capacities of all ZIFs at 77 K are smaller than that reported for some of MOF type materials, such as MOF-177 (10 wt.%) [1], and COF materials [3].

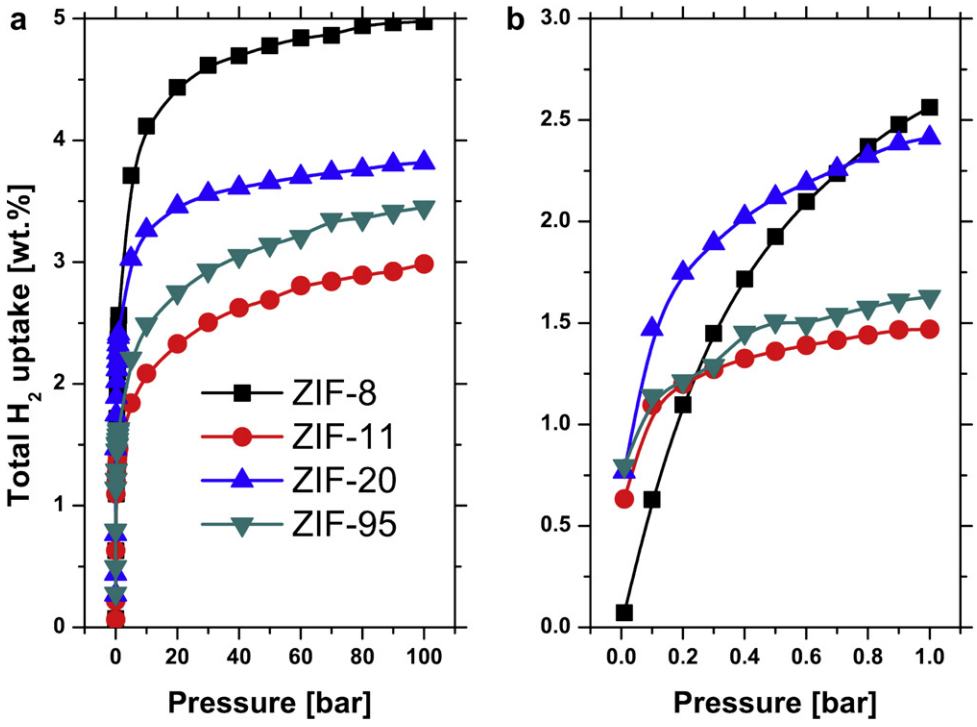

Fig. 9 – Theoretical hydrogen adsorption isotherms at 77 K and a) high pressure, b) low pressure from 0 to 1 bar.

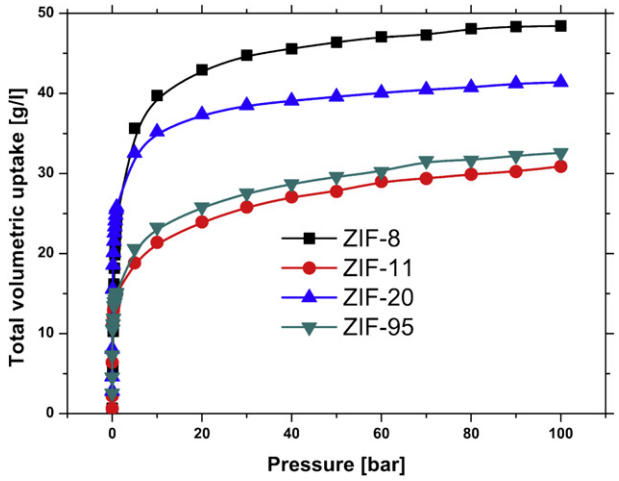

Fig. 10 – Theoretical volumetric isotherms of hydrogen adsorption at 77 K.

The volumetric storage capacities are shown in Fig. 10. Here ZIF-8 exhibits the highest uptake values too. The volumetric uptake of ZIFs, MOFs and COFs are of the same order of magnitude [38].

At room temperature all ZIF materials show similar gravimetric (less than 1.0 wt%) and volumetric uptakes of H_2 (see Fig. 11), comparable to that reported for some MOF type materials [30] and much smaller than that reported for COFs [3,38,39]. It is known that COFs can offer higher surface area and larger pore volume. Thus, towards a better adsorption capacity both at 77 and 300 K, new ZIF materials with higher surface and pore volume must be designed. This probably can be achieved either by investigating new topologies with lower density [40] or by substituting the metal atom in the structure by lighter elements (e.g. B or Li) [9,41–43].

Fig. 12 presents the calculated isosteric heats of adsorption Q_{st} for H_2 at 77 K in ZIFs. ZIF-95 has the highest heat of adsorption comparable to that of ZIF-11 and ZIF-20. This higher adsorption energy is responsible for the higher H_2 storage at low pressure. The maximum heat of adsorption for ZIFs varies between 12.0 kJ/mol (ZIF-95), 10.5 kJ/mol (ZIF-20), 9.8 kJ/mol ZIF-11 and 5.9 kJ/mol for ZIF-8. The heats of adsorption of ZIF-95, –20 and ZIF-11 are relatively high compared with other porous materials [44], such as, MOFs with small pores [45]. We note that the calculated isosteric heat of adsorption of ZIF-8 and ZIF-20 are in good agreement with those determined from the experiment (4.5 kJ/mol for ZIF-8 [15] and 8.5 kJ/mol for ZIF-20 [12]). Moreover, the calculated heat of adsorption of ZIF-8 and ZIF-11 agree well with those reported in our previous work using DC-DFTB (6.9 kJ/mol for ZIF-8 and 10.23 kJ/mol for ZIF-11) [27]. The presence of bIM in ZIF-11, Pur in ZIF-20 and cbIM in ZIF-95 leads to enhanced adsorption energy comparing to ZIF-8. Moreover, the presence of Cl in cbIM leads to limited increase of the adsorption energy compared to bIM and Pur. However, the Cl atom is much heavier than H which leads to a decrease in the hydrogen capacity of ZIF-95 compared to ZIF-20. On the other hand the presence of N in Pur linker leads to an increase of the adsorption energy compared to bIM linker (Fig. 12). This is consistent with previous theoretical investigations indicating that nitrogen heterocycles (e.g. pyrazine) can enhance the adsorption energy of H_2 [46]. The presented analysis also suggests to utilize purinate as a preferred linker when designing new ZIF type materials for hydrogen storage applications.

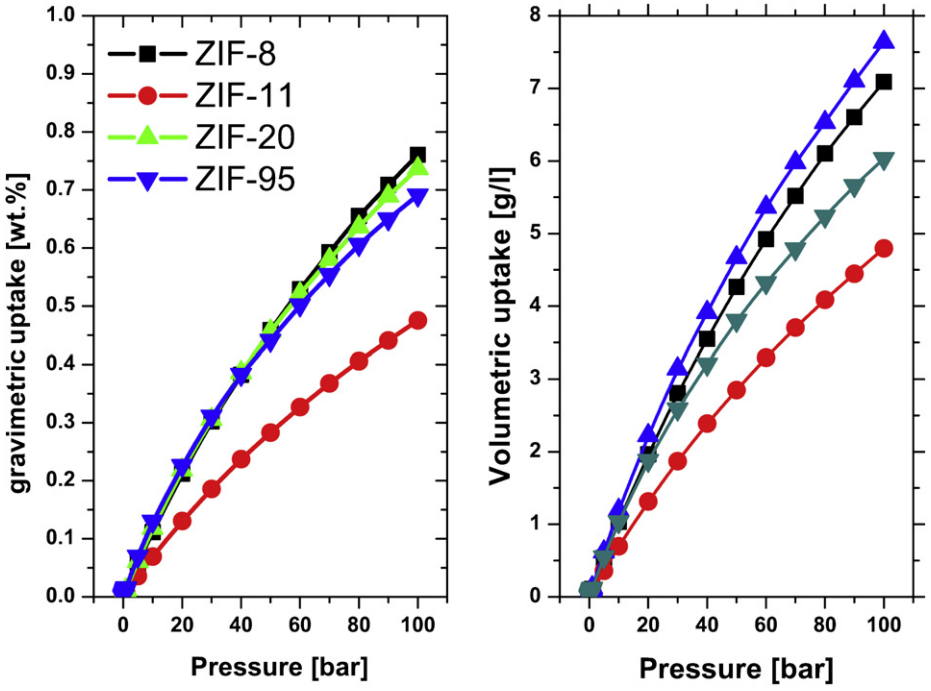

Fig. 11 – Theoretical gravimetric and volumetric isotherms of hydrogen adsorption at 300 K for ZIFs.

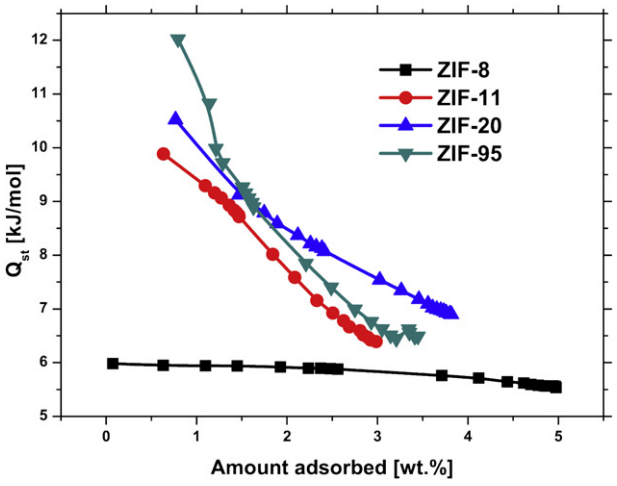

Fig. 12 – Calculated heats of adsorption for hydrogen in ZIFs at 77K.

4. Summary and conclusions

In this work hydrogen adsorption in nanoporous ZIFs was investigated as a function of network geometry and organic linker exchange. To achieve a modeling free from any reference to specific ZIFs, accurate interaction energies were calculated based on the MP2 level. These energies were coarse-grained into a force field and then employed in classical GCMC calculations to obtain accurate H_2 uptake curves under different thermodynamic conditions. The calculated curves provide a benchmark for a nominal H_2 uptake, useful for reliably contrasting experimental results, which are often affected by material artifacts or experimental setup casualties.

The total hydrogen uptake of ZIF-8 at moderate and high pressure (>10 bar) was found to amount ~5 wt.%, higher than other ZIF materials. This is due to higher surface area and larger free volume. At lower pressures ZIF-20 was found to overperform other ZIF materials due to its higher heat of adsorption.

The positive effect of nitrogen heterocycle ligands on the hydrogen uptake was attributed to an enhanced adsorption energy, which is larger for ZIF-20 (Purinate ligand) than for ZIF-11 (bIM ligand). Hydrogen substitution by chlorine in the organic rings has only moderate impact on adsorption energy at the cost of a lower hydrogen capacity.

All in all, benchmark H_2 uptake values and adsorption energy based on MP2 have been presented for a class of ZIF compounds, with different topologies and ligands. We understand our computational scheme as a transferable approach for the evaluation and screening of material properties, and for improved material design.

Acknowledgment

This work was supported by the Deutsche Forschungsgemeinschaft via the priority program 'Metal-Organic Framework'. We thank ZIH Dresden for the computational support.

REFERENCES

[1] Wong-Foy AG, Matzger AJ, Yaghi OM. Exceptional H_2 saturation uptake in microporous metal-organic frameworks. J Am Chem Soc 2006;128:3494–5.
[2] El-Kaderi HM, Hunt JR, Mendoza-Cortes JL, Cote AP, Taylor RE, O'Keeffe M, et al. Designed synthesis of 3D covalent organic frameworks. Science 2007;316:268–72.
[3] Han SS, Furukawa H, Yaghi OM, Goddard WA. Covalent organic frameworks as exceptional hydrogen storage materials. J Am Chem Soc 2008;130:11580–1.
[4] Park SJ, Lee SY. Hydrogen storage behaviors of platinum-supported multi-walled carbon nanotubes. Int J Hydrogen Energy 2010;35:13048–54.
[5] Reguera L, Roque J, Hernandez J, Reguera E. High density hydrogen storage in nanocavities: role of the electrostatic interaction. Int J Hydrogen Energy 2010;35:12864–9.
[6] Maark TA, Pal S. A model study of effect of m = Li+, Na+, Be2+, Mg2+, and Al3+ ion decoration on hydrogen adsorption of metal-organic framework-5. Int J Hydrogen Energy 2010;35:12846–57.
[7] Khvostikova O, Assfour B, Seifert G, Hermann H, Horst A, Ehrenberg H. Novel experimental methods for assessment of hydrogen storage capacity and modelling of sorption in Cu-BTC. Int J Hydrogen Energy 2010;35:11042–51.
[8] Assfour B, Seifert G. Adsorption of hydrogen in covalent organic frameworks: comparison of simulations and experiments. Microporous Mesoporous Mater 2010a;133:59–65.
[9] Baburin IA, Assfour B, Seifert G, Leoni S. Polymorphs of lithium-boron imidazolates: energy landscape and hydrogen storage properties. Dalton Trans; 2011. doi:10.1039/C0DT01441A.
[10] Park KS, Ni Z, Cote AP, Choi JY, Huang RD, Uribe-Romo FJ, et al. Exceptional chemical and thermal stability of zeolitic imidazolate frameworks. Proc Natl Acad Sci USA 2006;103:10186–91.
[11] Huang XC, Lin YY, Zhang JP, Chen XM. Ligand-directed strategy for zeolite-type metal-organic frameworks: zinc(II) imidazolates with unusual zeolitic topologies. Angew Chem Int Ed 2006;45:1557–9.
[12] Hayashi H, Cote AP, Furukawa H, O'Keeffe M, Yaghi OM. Zeolite a imidazolate frameworks. Nat Mater 2007;6:501–6.
[13] Wang B, Cote AP, Furukawa H, O'Keeffe M, Yaghi OM. Colossal cages in zeolitic imidazolate frameworks as selective carbon dioxide reservoirs. Nature 2008;453:207–11.
[14] Wu H, Zhou W, Yildirim T. Hydrogen storage in a prototypical zeolitic imidazolate framework-8. J Am Chem Soc 2007;129:5314–5.
[15] Zhou W, Wu H, Hartman MR, Yildirim T. Hydrogen and methane adsorption in metal-organic frameworks: a high-pressure volumetric study. J Phys Chem C 2007;111:16131–7.
[16] Zhou M, Wang Q, Zhang L, Liu YC, Kang Y. Adsorption sites of hydrogen in zeolitic imidazolate frameworks. J Phys Chem B 2009;113:11049–53.
[17] Mayo SL, Olafson BD, Goddard WA. Dreiding: a generic force field for molecular simulations. J Phys Chem 1990;94:8897–909.
[18] Jorgensen WL, Maxwell DS, Tirado-Rives J. Development and testing of the OPLS All-Atom force field on conformational energetics and properties of organic liquids. J Am Chem Soc 1996;118:11225–36.
[19] Fischer M, Hoffmann F, Froba M. Preferred hydrogen adsorption sites in various MOFs–a comparative computational study. ChemPhysChem 2009;10:2647–57.
[20] Han SS, Choi SH, Goddard WA. Zeolitic imidazolate frameworks as H_2 adsorbents: Ab initio based grand canonical monte carlo simulation. J Phys Chem C 2010;114:12039–47.

[21] Møller C, Plesset MS. Note on an approximation treatment for many-electron systems. Phys Rev 1934;46:618–22.
[22] Kristyan S, Pulay P. Can (semi)local density-functional theory account for the London dispersion forces. Chem Phys Lett 1994;229(3):175–80.
[23] Dunning Jr TH. Gaussian basis sets for use in correlated molecular calculations. I. The atoms boron through neon and hydrogen. J Chem Phys 1989;90:1007–23.
[24] Hubner O, Gloss A, Fichtner M, Klopper W. On the interaction of dihydrogen with aromatic systems. J Phys Chem A 2004; 108:3019–23.
[25] Heine T, Zhechkov L, Seifert G. Hydrogen storage by physisorption on nanostructured graphite platelets. Phys Chem Chem Phys 2004;6:980–4.
[26] Assfour B, Seifert G. Hydrogen adsorption sites and energies in 2D and 3D covalent organic frameworks. Chem Phys Lett 2010b;489:86–91.
[27] Assfour B, Leoni S, Seifert G. Hydrogen adsorption sites in zeolite imidazolate frameworks ZIF-8 and ZIF-11. J Phys Chem C; 2010:13381–4.
[28] Frisch MJ, Trucks GW, Schlegel HB, Scuseria GE, Robb MA, Cheeseman JR, et al. Gaussian 03, Revision C.03. Wallingford, CT: Gaussian, Inc.; 2004.
[29] Cao D, Lan J, Wang W, Smit B. Lithium-doped 3d covalent organic frameworks: high-capacity hydrogen storage materials. Angew Chem Int Ed 2009;121:4824–7.
[30] Yang Q, Zhong C. Molecular simulation of adsorption and diffusion of hydrogen in metalâ'organic frameworks. J Phys Chem B 2005;109:11862–4.
[31] Surble S, Millange F, Serre C, Düren T, Latroche M, Bourrelly S, et al. Synthesis of MIL-102, a chromium carboxylate metal-organic framework, with gas sorption analysis. J Am Chem Soc 2006;128:14889–96.
[32] Gupta A, Chempath S, Sanborn MJ, Clark LA, Snurr RQ. Object-oriented programming paradigms for molecular modeling. Mol Simul 2003;29:29–46.
[33] Frost H, Düren T, Snurr RQ. Effects of surface area, free volume, and heat of adsorption on hydrogen uptake in metal-organic frameworks. J Phys Chem B 2006;110:9565–70.
[34] Assfour B, Seifert G. Hydrogen storage in 1D nanotube-like channels metal-organic frameworks: effects of free volume and heat of adsorption on hydrogen uptake. Int J Hydrogen Energy 2009;34:8135–43.
[35] Düren T, Millange F, Férey G, Walton KS, Snurr RQ. Calculating geometric surface areas as a characterization tool for metalâ'organic frameworks. J Phys Chem C 2007;111: 15350–6.
[36] Liu J, Culp JT, Natesakhawat S, Bockrath BC, Zande B, Sankar SG, et al. Experimental and theoretical studies of gas adsorption in Cu3(BTC)2: an effective activation procedure. J Phys Chem C 2007;111:9305–13.
[37] Garberoglio G, Skoulidas AI, Johnson JK. Adsorption of gases in metal organic materials: comparison of simulations and experiments. J Phys Chem B 2005;109:13094–103.
[38] Klontzas E, Tylianakis E, Froudakis GE. Hydrogen storage in 3D covalent organic frameworks. A multiscale theoretical investigation. J Phys Chem C 2008;112:9095–8.
[39] Garberoglio G. Computer simulation of the adsorption of light gases in covalent organic frameworks. Langmuir 2007; 23:12154–8.
[40] Baburin IA, Leoni S, Seifert G. Enumeration of not-yet-synthesized zeolitic zinc imidazolate MOF networks: a topological and DFT approach. J Phys Chem B 2008;112: 9437–43.
[41] Wu T, Zhang J, Zhou C, Wang L, Bu XH, Feng PY. Zeolite rho-type net with the lightest elements. J Am Chem Soc 2009a; 131:6111–3.
[42] Wu T, Zhang J, Bu XH, Feng PY. Variable lithium coordination modes in two- and three-dimensional lithium boron imidazolate frameworks. Chem Mater 2009b;21:3830–7.
[43] Chen SM, Zhang J, Wu T, Feng PY, Bu XH. Zinc(ii)-boron(iii)-imidazolate framework (ZBIF) with unusual pentagonal channels prepared from deep eutectic solvent. Dalton Trans 2010;39:697–9.
[44] Rowsell JLC, Yaghi OM. Effects of functionalization, catenation, and variation of the metal oxide and organic linking units on the low-pressure hydrogen adsorption properties of metal-organic frameworks. J Am Chem Soc 2006;128:1304–15.
[45] Dinca M, Yu AF, Long JR. Microporous metal-organic frameworks incorporating 1,4-benzeneditetrazolate: syntheses, structures, and hydrogen storage properties. J Am Chem Soc 2006;128:8904–13.
[46] Samanta A, Furuta T, Li J. Theoretical assessment of the elastic constants and hydrogen storage capacity of some metal-organic framework materials. J Chem Phys 2006;125:084714–8.